Escola Tècnica Superior d'Enginyeries Industrial i Aeronàutica de Terrassa

UNIVERSITAT POLITÈCNICA DE CATALUNYA

Study of the performance of an inertial measurement unit on board a launcher

- ANNEX A -

Description of the most relevant sensor types

Author: Xavier Laguna Benet

Tutors: Gisela Detrell Domingo (ETSEIAT),
Elena Fantino (ETSEIAT)
Collaborator: Eduard Diez Lledó (GTD)

Enginyeria Superior Aeronàutica

March 2014

Index and list of abreviations

Acronyms and symbols

AIG	atomic interferometer gyroscope
ASG	atomic spin gyroscope
DART	dual axis rate transducer
DC	direct current
ESAM	electron spin angle momentum
EPS	electrical power system
f	frequency
FOG	fibre optic gyroscope
Gyro	gyroscope
h	hour
INS	inertial navigation system
ISA	inertial sensor assembly
LPF	Larmor precession frequency
MEMS	micro-electromechanical system(s)
MWG	momentum wheel gyroscope
NMR	nuclear magnetic resonance
NSAM	nuclear spin angle momentum
TCS	thermal control system
TRL	technology readiness level

IN EQUATIONS

$a_{coriolis}$	Acceleration produced by the Coriolis effect.
Δθ	Angle variation. The turning angle depends on the context.
V_{rot}	Velocity in the rotating frame
ω	Angular velocity of the rotating frame

List of figures

List of tables

A.1 Introduction

The aim of this annex is to offer background theory and information on sensors and sensing error modelling. Although some sensor types do not fulfil the basic requirements for being utilised in the Aldebaran demonstrator, the basic sensor types are illustrated aiming at providing a global view on sensors.

A.2 Gyroscope types

The first gyroscope sensor was built by Jean Bernard Léon Foucault to demonstrate experimentally the rotation of the Earth [A-3]. The concept consists in giving angular momentum to an object. If there are no torques applied to this object, the angular momentum stays constant. Momentum wheel gyroscopes (MWGs) are devices of this kind. They tend to be heavy and big. For example, the sensor invented by Foucault was 68 m high and weighed 25 Kg[A-3]. Later gyroscopes were considerably smaller and lighter.

At the beginning of the twentieth century, magnetic compasses caused many problems in navigation when the host vehicles were metallic. Therefore, gyrocompasses were developed. The concept is the same as a MWG with a torque applied when the MWG is not pointing towards the North. There are basically two ways of doing it, by friction or by confining it in the horizontal plane. The first way consists in submerging the MWG in a fluid that applies a torque when the MWG turns. By taking into account the Earth's rotation and the precession, it can be deduced that the gyrocompass will tend to point towards the true North. The other method consists in fixing the gyroscope axis in a horizontal plane and letting free the motion in the plane. As in the previous case, when the MWG is not pointing to the true North, a force that pushes the MWG to the true North by means of precession appears. In this case the force is gravity. However, such gyrocompass drift is very large in the case of ships due to the roll produced by the waves. The solution proposed by Maximilian Schuler was to join the gyrocompass with an elastic material. The concept is to adjust the natural frequency of the system to the frequency of a hypothetical satellite at sea level (84.4 minutes period).

A.2.1 Coriolis torque feedback gyroscopes

Torque feedback gyroscopes use a servo loop to maintain the momentum wheel in the same orientation with respect to the host vehicle. The feedback torque is very well defined. As a consequence, the displacement $\Delta\theta$ produced at each pulse is known. By knowing the number of pulses in a given time interval, allows to compute the corresponding turning angle. However, the quantization error for the measured angle and the precision of the applied torque have to be taken into account.

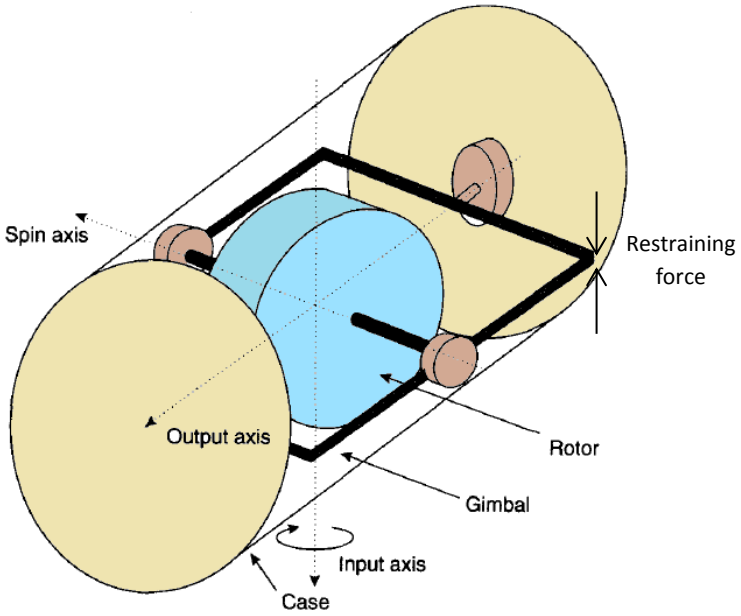

Figure 1: Torque feedback gyroscope with one measuring direction[A-1].

As shown in Figure 1, this gyro is based on the Coriolis effect.

$$\mathbf{a_{coriolis}} = -2 \cdot (\boldsymbol{\omega} \times \mathbf{V_{rot}}). \qquad \textbf{Eq. 1}$$

This effect is seen as an acceleration felt by an object fixed with a rotating coordinate system. In Eq. 1 the elements involved in the vector cross product are the coordinate rotation rate vector and the velocity of the body as measured in the rotating reference frame. It must be stressed that precession and Coriolis effect are two aspects of the same phenomenon. The Coriolis acceleration is a consequence of the precession of the body.

This type of accelerometers can produce two types of output. One type consists in using some sort of restraining system (a restraining spring, for example) thus allowing the turning angle around the output axis to be measured. The other type uses a restraining force to avoid the turning around output axis. The number of impulses sent to the force actuator constitutes the sensor output.

Coriolis torque feedback gyroscopes gyroscope is also known as rate-integrating gyroscope because the output is proportional to the attitude change and not to the attitude rate change as in some others gyros.

The signal of this gyroscope is given by:

$$\widetilde{\omega_x} = (1 + S_x)\omega_x + M_y\omega_y + M_z\omega_z + B_{fx} + B_{gx}a_x + B_{gz}a_z + B_{axz}a_xa_z + n_x, \qquad \textbf{Eq. 2}$$

where:

$\widetilde{\omega_x}$ is the signal output divided by the nominal scale factor
B_{fx} is the g-insensitive bias
$B_{gx,z}$ are the g-sensitive coefficients
B_{axz} is the anisoelasic bias coefficient
n_x is the zero-mean random bias
$M_{y,z}$ are the cross coupling coefficients
S_x is the scale-factor error

A.2.2 Rotating Coriolis multi-sensor

The following gyroscope types are based on the Coriolis effect. The rotating Coriolis gyroscope is a bidirectional gyroscope. It consists in a momentum wheel with a gyroscope mounted with the measurement axis parallel to the rotation axis. The basic gyroscope scheme is represented in Figure 2.

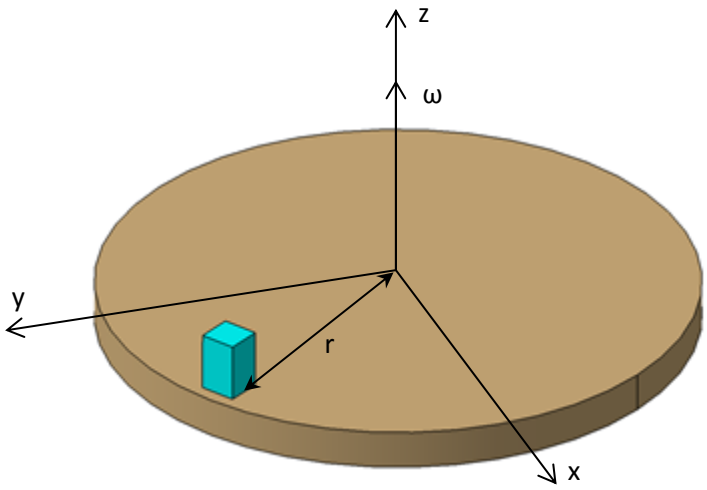

Figure 2: Basic rotating Coriolis gyroscope scheme.

If an attitude rate perturbation occurs, for example Ω, the accelerometer sensed acceleration is:

$$\mathbf{a_{coriolis}} = -2 \cdot \left(\begin{bmatrix} \Omega_x \\ \Omega_y \\ \Omega_z \end{bmatrix} \mathrm{x} \begin{bmatrix} -r \cdot \omega \cdot \sin(\omega t) \\ r \cdot \omega \cdot \cos(\omega t) \\ 0 \end{bmatrix} \right) = \begin{bmatrix} - \\ - \\ -2 \cdot r \cdot \omega \cdot \left[\Omega_x \cdot \cos(\omega t) + \Omega_y \sin(\omega t) \right] \end{bmatrix}, \quad \textbf{Eq. 3}$$

where:

$a_{coriolis}$ is the Coriolis acceleration
Ω_i is the attitude rate perturbation in the i axis

r is the distance between the sensor and the spinning axis
ω is the nominal angular velocity
t is the time past from sensor last alignment with the x axis
– are the Coriolis acceleration terms that are not interesting for this study

The accelerometer sensed acceleration is equal and opposite to the acceleration found in Eq. 3.

The output signal of the accelerometer can be demodulated and then Ω_y and Ω_x can be obtained. The demodulation process deletes any DC bias. As a consequence, there is no need of calibrating the sensor with respect to bias error.

This design can be transformed in a rotating multi-sensor by adding an accelerometer to the momentum wheel with a measurement axis orthogonal to the spin axis like in Figure 3.

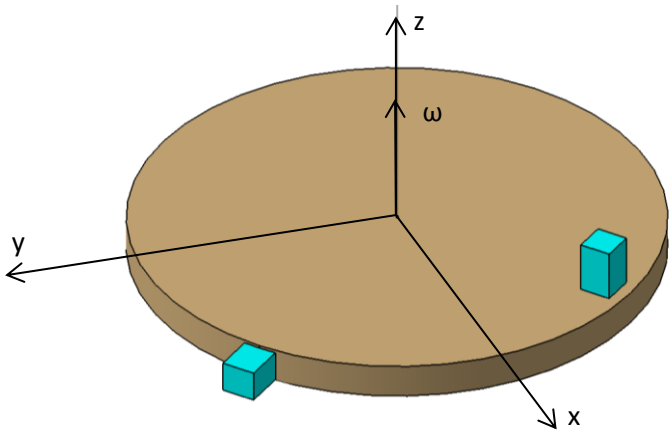

Figure 3: Rotating multi-sensor.

With this design, a bidirectional accelerometer and a bidirectional gyroscope with no effective bias error can be obtained. Obviously, the output signal of the added accelerometer also needs to be demodulated in a similar way as the first accelerometer.

This kind of gyroscope has the problem of nutation. The nutation is self-sustained and consists in a wobbling of the spin axis of the momentum wheel. The nutation frequency, ω_R, depends on the angular momentum (H), the rotor and inner structure moment of inertia about the inner gimbal structure axis (I_{1g}) and the rotor and inner and intermediate structure moment of inertia about the outer axis (I_{2g}):

$$\omega_R = \frac{H}{\sqrt{I_{1g} I_{2g}}} . \qquad \text{Eq. 4}$$

In a non-frictional system the nutation would be infinite. But gimbals and structure drag reduce nutation. Sometimes, some viscous drag elements are added in order to dissipate faster. In order for this to happen, the nutation frequency should be as high as possible. The ratio between the inertia moment of the momentum wheel and the other structures should be as large as possible and the momentum wheel turn velocity should also be as high as possible.

A variant of this configuration is the dynamically tuned gyroscope. This gyroscope is not equipped with accelerometers. These are feedback type gyros. As it can be seen in Figure 4, the sensor size is considerably reduced compared to the rotating Coriolis multisensor.

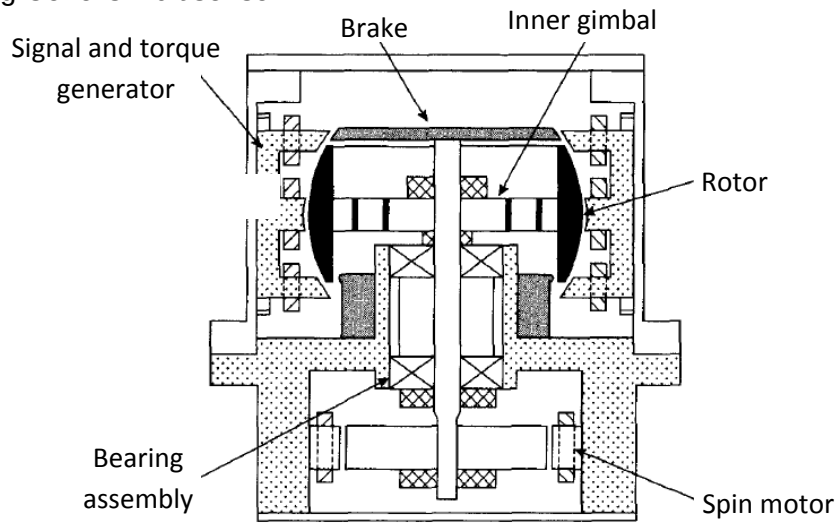

Figure 4: Tuned rotor gyroscope configuration[A-1].

The rotor is connected to the drive shaft by a pair of hinges. They can be flexure hinges. In this way, angular momentum is transmitted to the rotor and the rotor has sufficient freedom for this application.

Usually, the decoupling is quite difficult to implement. Therefore, the system uses a torsional spring and the motion reduces to small deviations. The torque feedback corrections are applied in two orthogonal directions. In this design it has to be taken into account that oscillations and harmonics of the natural frequency can perturb the measurements. If the ISA (inertial sensor assembly) is intended for being installed in a vehicle where these frequencies can be expected, it must be made sure that these vibrations are not transmitted to the ISA.

Angular rate measurements are carried out as Eq. 2 indicates for both directions.

The Flex gyroscope is a reduced variant of the dynamically tuned gyros. The difference lies in the absence of the pair of hinges that connect the rotor and the drive shaft. The flex gyroscope uses a flexure pivot. Usually, this arrangement is

made by using a spider and strut configuration. As most configurations, it introduces some torques. These torques are compensated by means of small magnets which are connected to high permeability screws placed in a plate that moves with the shaft.

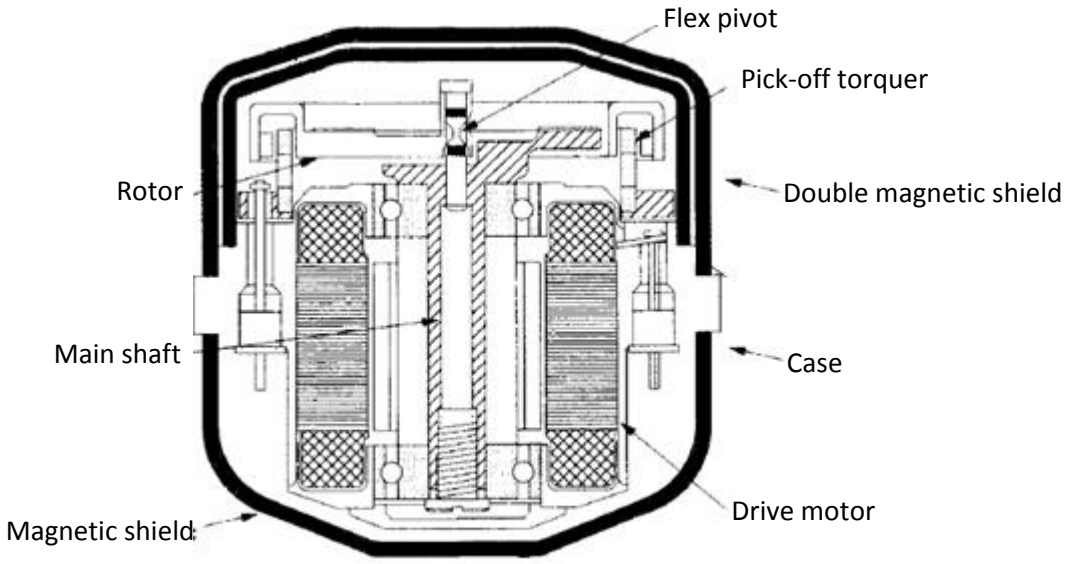

Figure 5: Flex gyroscope[A-1].

As illustrated in Figure 5, the magnetic solution for compensating undesired torques has a drawback. The gyroscope needs to be magnetically isolated. As no isolation is perfect, the gyroscope will be magnetically sensible and the performance will get worse when the gyroscope is subjected to a magnetic field.

A.2.3 Dual axis rate transducer (DART)

This gyroscope is also based on precession. It consists in a heavy-density liquid contained in a spherical cavity which rotates at high speeds. Inside this cavity there is an assembly of paddles with piezoelectric crystals on the sides. The spherical cavity is spinning, but does not have any other degree of freedom respect to the gyro case. When the gyro turns around a vector contained in the input axis plane, the rotation is transmitted to the cavity and a torque is damped by the fluid due to viscosity. The fluid then precesses at the input rate.

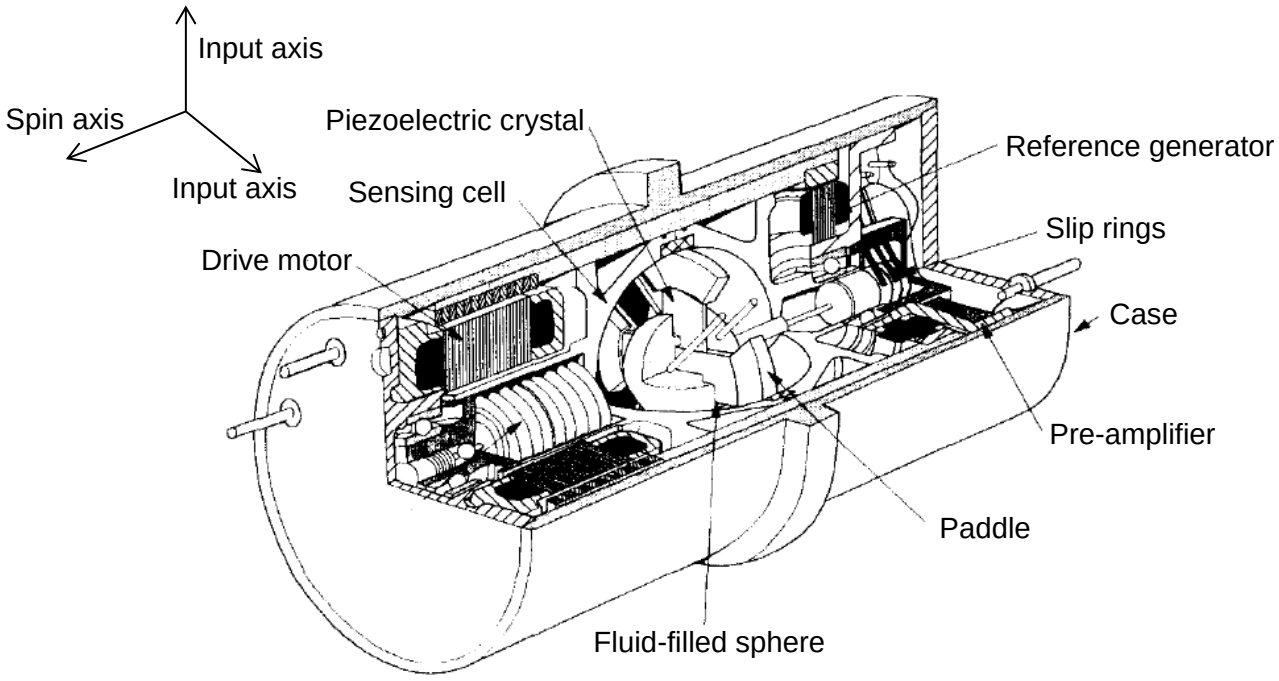

Figure 6: DART[A-1]

When the fluid precesses, it creates a pressure distribution to the paddles that the piezoelectric crystals convert to electrical signals. With the electrical signals distribution, the angular rate in measurement plane axis can be known.

A.2.4 Laser gyroscopes

Laser gyroscopes are based on the Sagnac effect. This effect is derived from the invariance of the speed of light. If a device similar to that represented in Figure 7 is mounted in a rotating host vehicle, the distance travelled by the clockwise and the anticlockwise light beams is different due to the rotation of the corner mirrors. The signal phase of the two beams at the detector is different and is a function of the angular velocity around the axis perpendicular to the plane that contains the laser beams trajectory.

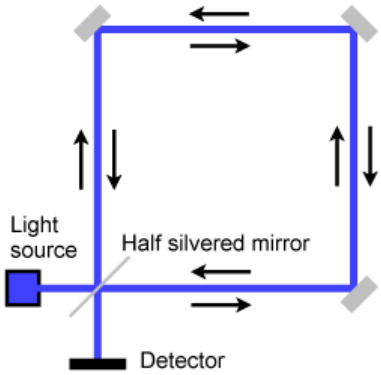

Figure 7: Schematic representation of a Sagnac interferometer.

The most important advantage of laser gyroscopes is the absence of moving parts. But this design (Ring Laser Gyroscope) does not operate properly near zero twirling values. This happens because the two beams cancel themselves. The solution found was the Zero Lock Ring Laser Gyroscope. This gyroscope uses frequency splitting and out of plane path segments to eliminate the cancelation.

The Fiberoptic Gyroscopes (FOGs) use the same principle than the Ring Laser Gyros. But in this case the signal is guided through an optical fiber. In order to increase the phase sensitivity, the optical fiber makes thousands of turns around the measurement axis. The Open-loop FOGs are based on the comparison of two counter-rotating beams. These gyros typically have sensitivities of 10^{-2} deg/h, bias stabilities of 1 deg/h and dynamic ranges of 10^3. An improvement of these gyros is the Closed-loop Integrating FOGs. In this case, the output phase is used to control a loop modulator that nulls the output. This gyros typically have dynamic ranges of 10^6, non-linearity errors of 10^{-5} and bias stabilities of 10^{-2} deg/h[A-4].

Optical gyros have the advantage of having a wide dynamic range, having an instant start-up. They are insensitive to environmental conditions, easily self-tested and they have high data rate capability.

A.2.5 Vibratory Coriolis Gyros

These gyros are based on the Coriolis effect on a particle that is moving in an oscillatory trajectory. The acceleration that the particle feels due to the Coriolis effect is:

$$a_{coriolis} = -2 \cdot (\Omega \times V_0) \cdot \cos(\Omega_{rot} t). \qquad \textbf{Eq. 5}$$

As shown in Eq. 5, $a_{coriolis}$ has the same frequency as the particle motion. The main problem of these gyros is constituted by the vibrations caused by the host vehicle.

The tuning fork gyroscope has two tines moving at the same time apart and together. By this way, the effect of host vehicle vibrations is cancelled or at least minimized.

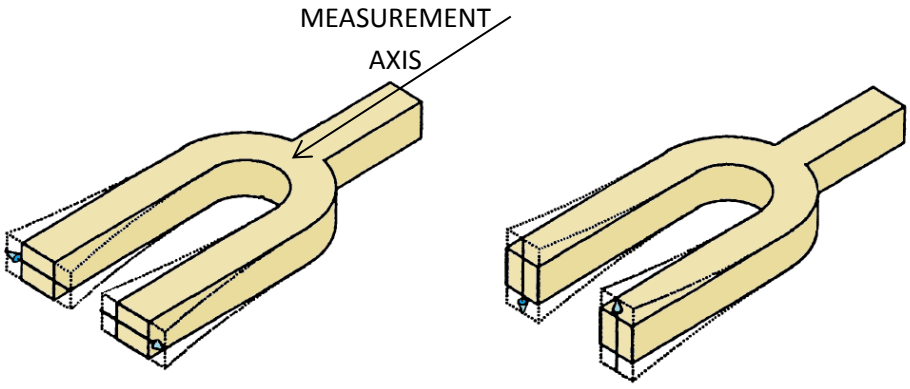

Figure 8: Vibration modes of a tuning fork gyroscope: input vibrating mode (right) and output vibration mode (left) [A-3]

The quartz rate sensor is a modification of the tuning fork gyroscope that makes it usable in practice. The idea is to mount two coaxial and coplanar forks. One pair of tines is forced to vibrate and the Coriolis effect affects them. The second pair of tines (upper pair in Figure 9) absorbs the produced efforts and vibrates perpendicularly to the first pair. This vibration is proportional to the turning rate around the fork axis.

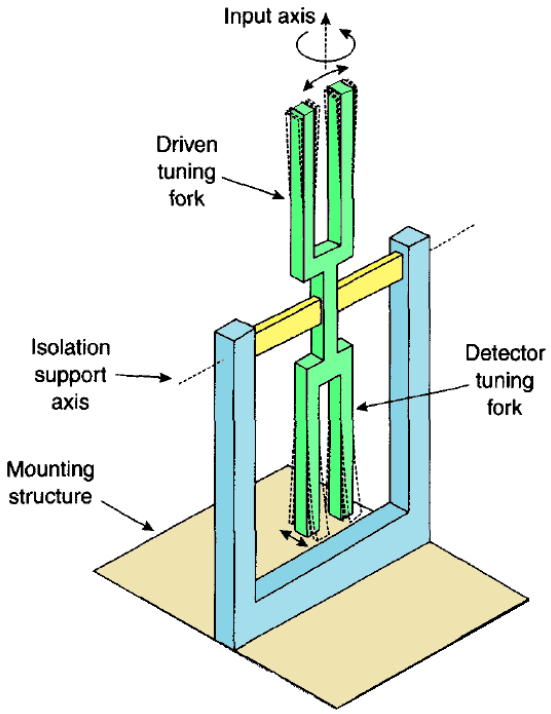

Figure 9: Quartz rate sensor [A-1]

The vibrations of the driven tuning fork are measured with a capacitive sensor. The detector tuning fork is forced to vibrate at its resonant frequency, usually around 10 Kz. This sensor has a very versatile design and can be adapted to many different applications. It can be implemented also with MEMS. The configuration in MEMS devices is a little bit different, but uses the same principle.

The Hemispherical Resonator Gyro uses the same principle. This gyroscope has a bowl-shaped structure supported as shown in Figure 10.

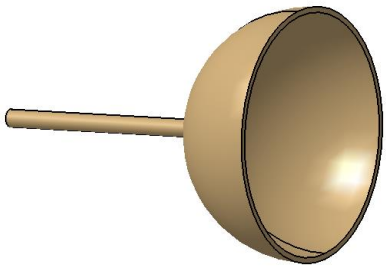

Figure 10: Hemispherical Resonator gyro.

Vibratory displacements normal to the edges of the bowl-shape are imposed. When the gyroscope is being rotated around the support axis, the nodes of the vibration modes rotate around the support. The rotation is proportional to the

input rotation rate. Like some other gyroscope designs, this gyroscope type has bad performance at low rotation rates.

The vibrating disc sensor also uses the same principle. But in this case a planar metal disc is used. The disc is supported by rigid spokes and it is forced to vibrate in a resonant sinusoidal oscillation in the disc plane.

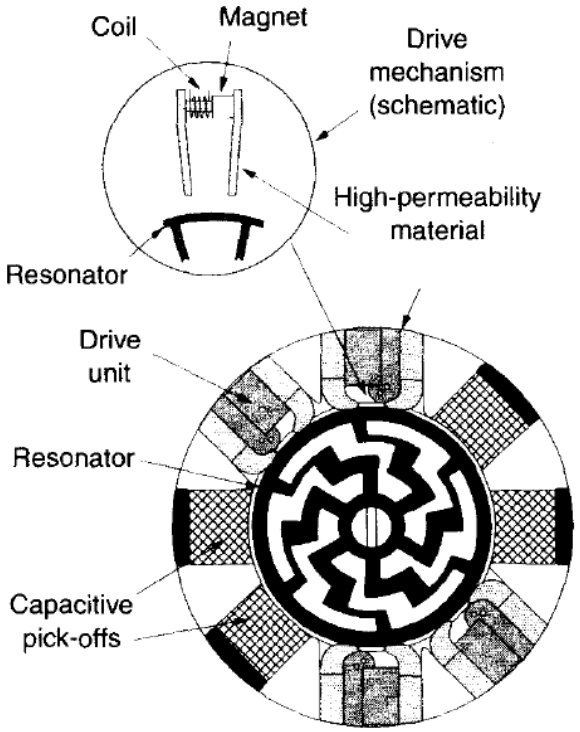

Figure 11: Vibrating disc gyro[A-1].

The motion of the ring is detected measuring the distance between a fixed plate and the edge of the ring by capacitive sensors. The operation is identical to the previously explained. The nodes and anti-nodes displacements are proportional to the angular rate around one of the input axis.

A.2.6 Silicon sensor

This gyro is very small (substantially less than 1mm). It is made with a very thin plate of single crystal silicon. This gyro has a double gimbal structure without any bearing; it is composed by two sets of flexible pivots. These flexible pivots allow rotation about their axis but they do not allow any other degree of freedom (ideally).

The outer electrodes are used to oscillate the inner part around the 'forced vibration axis', as shown in Figure 12. When there is angular rate around the

input axis, the inner part starts vibrating around the output axis at the same frequency and with amplitude proportional to the angular rate of the input axis.

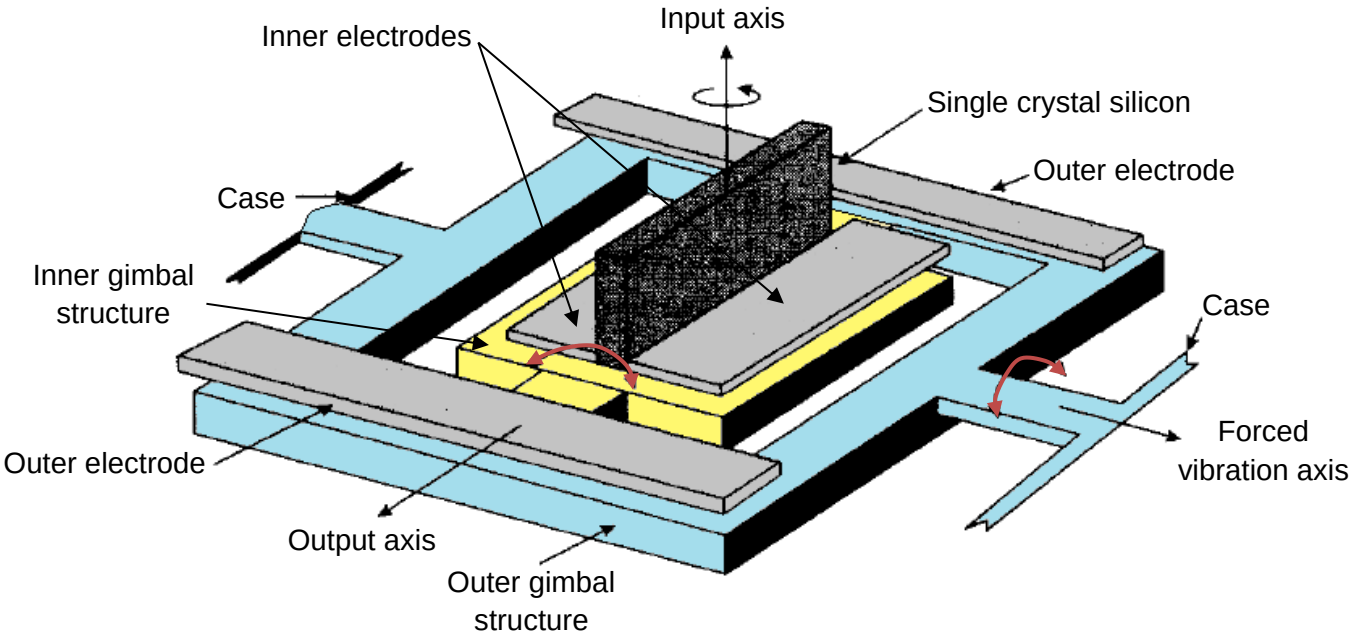

Figure 12: Silicon gyroscope[A-1].

The silicon is mounted perpendicularly to the 'forced vibration axis' and electroplated with gold. The outer inner electrodes detect the silicon movement. In order to achieve better performance, this gyro is implemented in closed-loop. The signal of the inner electrodes is used to control the compensation circuit that forces the inner part to stay almost stationary. The inner electrodes are used to do so. To prevent interferences, the measuring and re-balancing signals use difference frequencies.

A.2.7 Vibration wire rate sensor

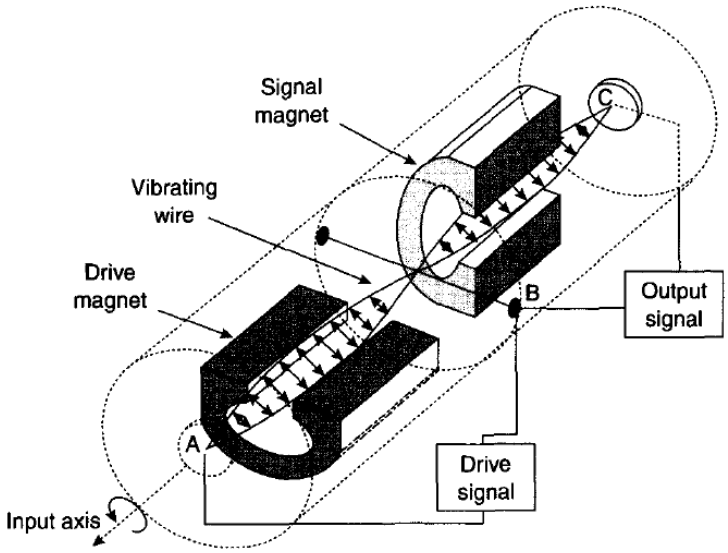

Figure 13: Vibrating wire rate sensor[A-1].

Figure 13 shows how a vibrating wire sensor operates. The conductive wire vibrates at the same frequency as the drive signal due to the magnetic field generated by the drive magnet. Behind the drive magnet, there is the signal magnet which creates a magnetic field orthogonal to the field of the drive magnet. The vibrating wire current is not affected by the signal magnet because the vibration plane and the electric field are orthogonal. But when the gyro has angular rate around the input axis, the vibrating plane tends to be maintained. Then, the signal magnet modifies the current. The difference between the input and the output signals is proportional to the angular rate.

The working frequency is usually around 20 KHz in order for the higher frequency signals, which can be produced by environmental vibrations, to be filtered out.

A.2.8 Cryogenic sensors

Cryogenic sensors are not going to be described in this project because they are not suitable for the Aldebaran demonstrator, although they could be the most precise gyroscopes. The nuclear magnetic resonance gyroscope and the SARDIN gyroscope have severe consequences on power consumption (Electrical Power System - EPS) and on the thermal control system (TCS). A rise in the TCS requirements implies a rise in the EPS requirements and consequently a weight increase. As the power it is going to be supplied by batteries, these EPS requirements increases mean bigger and heavier batteries. Therefore, these gyros are not suitable for launchers.

A.2.9 Electrostatically suspended gyroscope

This gyroscope consists in a ball turning at high speeds suspended by an electric field. This gyroscope has an extremely good performance, but it cannot work in high vibratory environments and even less in shock environments. These environments do not degrade the performance, but the gyroscope can be easily destroyed. As a consequence, this gyroscope is not going to be detailed in this project because it does not match the Aldebaran demonstrator requirements.

A.2.10 Fluidic

This type of gyroscope consists in a spherical cavity that contains a gas turning in a known direction. When the sensor turns with the host vehicle, the rotating gas keeps turning in the same direction. Then, the rotating direction difference can be measured by pressure differences or by hot wire anemometers.

Although this type of gyroscope sensor has been utilised for flight control, stabilisation and flight safety systems, it has not sufficient stability, resolution and environmental insensitivity to be used in navigation applications.

A.2.11 Fluxgate magnetometers

Fluxgate magnetometers gyros are composed by three orthogonal gyros. They measure the attitude respect to an external magnetic field. In navigation the magnetic field used is the Earth magnetic field. They are relatively cheap, small and reliable. But they cannot give by themselves complete attitude information. Although having a 0.1 degree resolution they are sometimes used as a reference because they present no drift.

Therefore, as they are not interesting to be used in the Aldebaran demonstrator context, fluxgate magnetometers are not going to be further detailed.

A.2.12 Atomic gyroscopes

There are two types of atomic gyroscopes: the Atomic Interferometer Gyroscope (AIG) and the Atomic Spin Gyroscope (ASG). AIG and ASG have been proved in the laboratory, but they have not been equipped in any host vehicle.

AIG systems have very good performance in the gravity direction, but in the horizontal direction the precision decreases dramatically. Although this performance decrease, the AIG horizontal precision is still much better than current gyroscope precision[A-6]. The reason why this type of gyroscope is not suitable in the context of the Aldebaran project is its size. The D.S. Durfee model

has a gyro length of two metres. This size can be reduced by changing the vibrating atom. Although improvements can be done in this way, in the near future a three axis gyroscope is not likely to be developed that could be contained in the volume shown in section 7.1 from the project report[A-5].

ASG is based on the fact that atomic spin keeps pointing at the same direction in inertial coordinate system. Since Nuclear Magnetic Resonance (NMR) technology is used for signal detection, the ASG gyroscope is also known as NMR gyroscope.

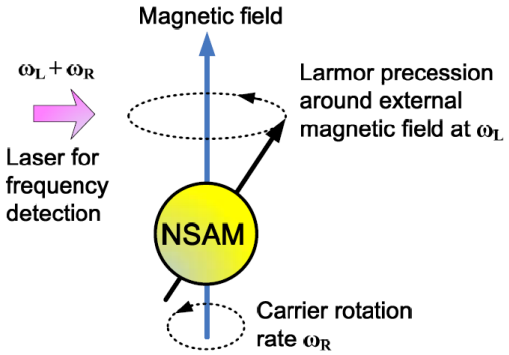

Figure 14: ASG principle of operation[A-5].

The nuclear spin angle momentum (NSAM) is going to precess around the magnetic field vector with a frequency called Larmor Precession Frequency (LPF). The LPF is constant depends on the atom and the magnetic field. Then, the laser detects the LPF and the sensor rotation rate sum.

In order to miniaturise this sensor, the concept has been slightly changed. The electron spin angular moment (ESAM) is fixed in inertial coordinate system if it is coupled with the NSAM of noble gas atoms. The magnetic field direction changes with the host vehicle and so does the sensor, while the ESAM stays fixed. This system can be implemented in MEMS. Although it has been tested in INS a few times, it is expected that in the near future. This system is expected to be relatively cheap[A-5].

A.2.13 Rotational Vibratory Coriolis Gyroscopes

Rotational Vibratory Coriolis Gyroscopes are MEMS devices. They consist in momentum wheels driven by an electrostatic rotational comb drive MEMS.

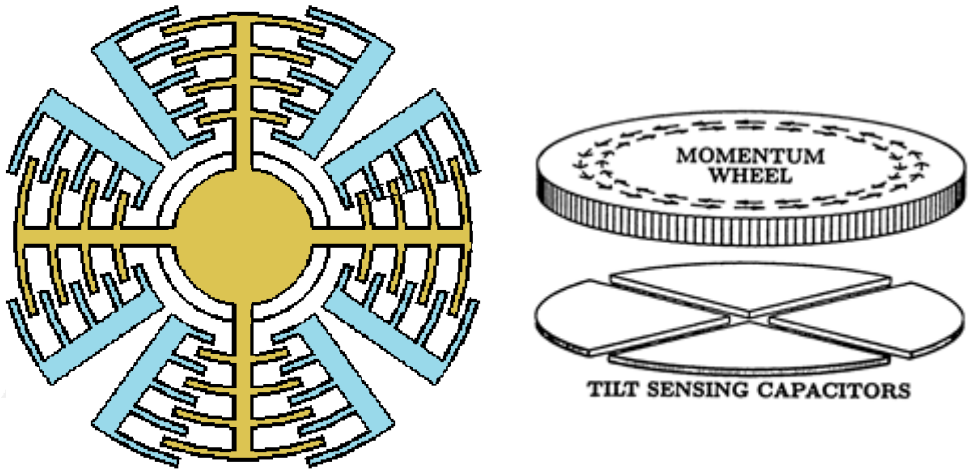

Figure 15: (left) Electrostatic rotational comb drive MEMS. Blue parts are fixed to the MEMS base and the brown part is the rotor. By applying potential differences between the rotor and the contiguous stator parts alternatively it can be achieved a sinusoidal angular momentum. (right) Rotational vibratory Coriolis gyro capacitors located under the momentum wheel. [A-3]

The rotational comb drive MEMS is connected to a torsion spring in order to simplify the design (more comb drive MEMS flexibility). If the momentum wheel is turned around any direction perpendicular to the momentum wheel axis, the momentum wheel will experience a sinusoidal tilting displaced by 90 degrees. This tilting can be sensed by for capacitors above or under the momentum wheel.

A.3 Types of accelerometers

An accelerometer is a device that measures acceleration. The first accelerometer was built at the beginning of the 19th century and was a pendulum. As the pendulum period equation depends on gravity, the pendulum period can be used to determine the gravity. This system is useful in static conditions, but in moving host vehicles it is useless.

A.3.1 Drag Cup Accelerometers

One of the first commercial accelerometers was the 'drag cup accelerometer'. This accelerometer consists in a magnetic bar and a drag cub, which is a nonferrous metal tube. When the magnetic bar is rotating, the induced currents in the tube produce a torque on it. In the accelerometer shown in Figure 16, the measurement axis is the vertical direction. The additional mass, which is fixed to the tube, produces a torque on the tube proportional to the acceleration. The engine that moves the magnetic bar acts in a way which depends on the tube position. The engine always tries to return the mass to its original position. As the magnetic bar's angular velocity is proportional to the torque made by the mass and the mass torque is proportional to the acceleration, the latter can be determined by measuring the power consumption in the engine.

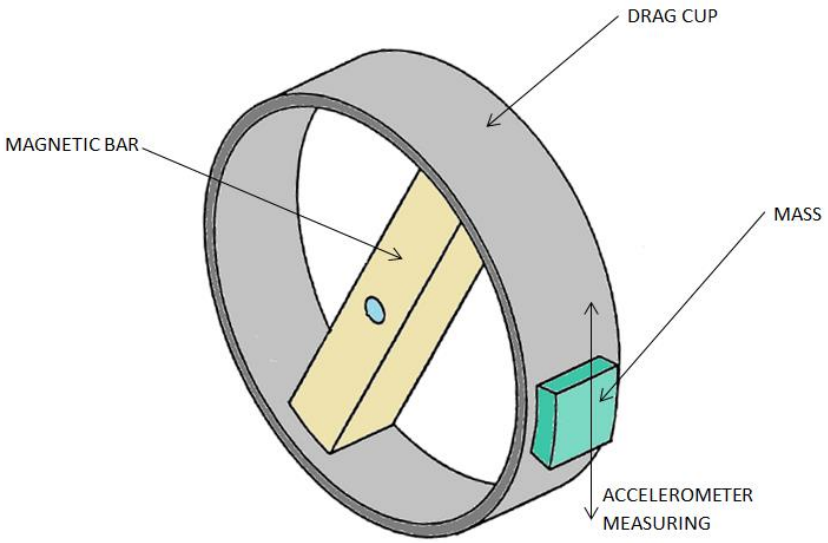

Figure 16: Scheme of a drag cup accelerometer.

A.3.2 Vibrating-Wire Accelerometer

The working principle of this accelerometer is based in the dependence of the resonance frequency of the wires on tension (they also depend on length, density and elastic modulus). With the configuration shown in Figure 17, the output signal frequency difference is a function of the acceleration. The frequency differences of the signals S1-S2, S3-S4 and S5-S6 can be analysed in order to determine the three axis acceleration.

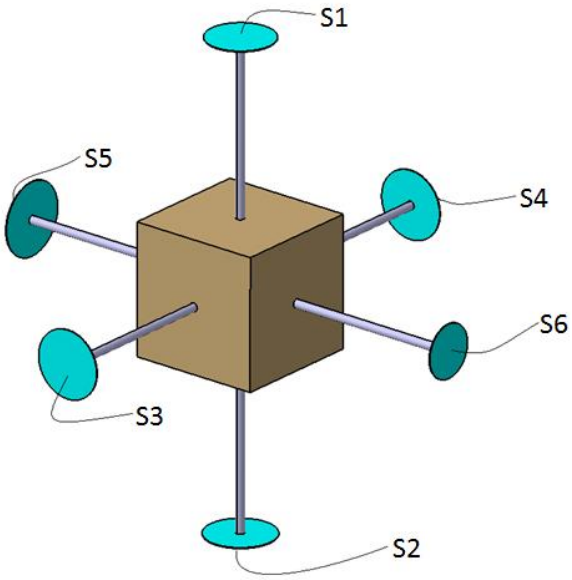

Figure 17: Scheme of a three axis vibrating-wire accelerometer. The blue parts represent the union between the wires and the fixed part to the host vehicle. The brown cube represents the suspended mass.

A.3.3 Gyroscopic accelerometers

The accelerometers types described previously are not competitive nowadays. One of the first accelerometers that are still used is the gyroscopic accelerometer. This accelerometer is based on precession. A momentum wheel is placed asymmetrically with respect to the supports with the aim of generating a torque perpendicular to the spin axis and to the acceleration. This torque is proportional to the acceleration. The precession makes the momentum wheel turn around the acceleration direction.

The torque feedback gyroscopic accelerometers are an improvement of the gyroscopic accelerometers. They consist in applying the same concept as in a torque feedback gyroscope but in a gyroscopic accelerometer. Therefore, the momentum wheel does not turn around the measurement axis. Then, the number

of impulses sent to the engine in order to maintain the spin axis fixed is proportional to the acceleration in the measurement axis.

A.3.4 Force feedback accelerometers

These accelerometers measure the force required to move a mass (proof mass) jointly with the host vehicle.

Electrostatic accelerometers leave the proof mass inside a cube surrounded by electrodes.

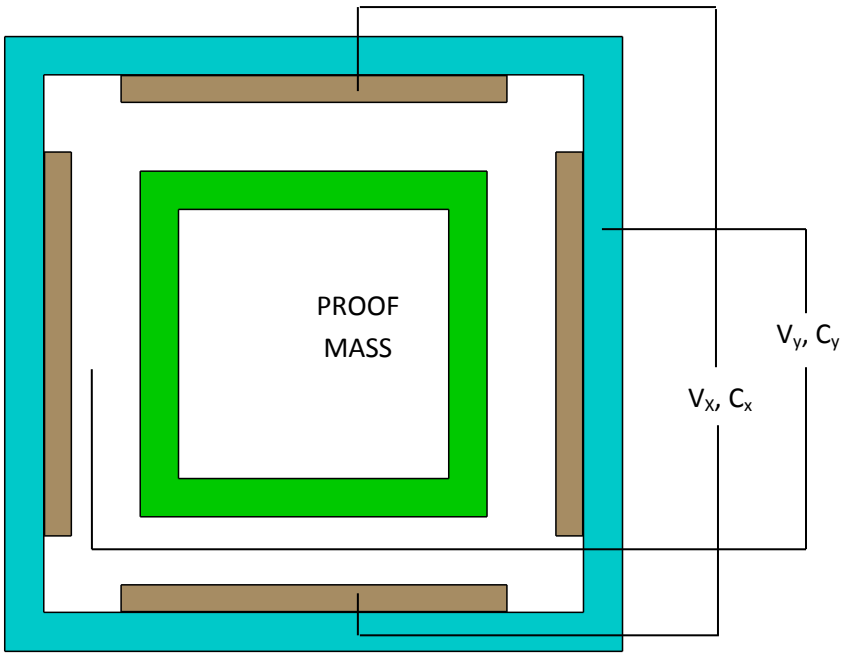

Figure 18: Three axis electrostatic accelerometer. The green part is the proof mass, the brown parts are the electrode plates and the blue part is the accelerometer sensor box.

The plate voltages suspend the mass so that it stays at the same distance from all the electrode plates. Measuring the capacitance of each plate to the cube provides the distance between the plate and the cube. By three servos (one per axis) the voltage variation needed to maintain a uniform gap can be obtained.

Pendulous accelerometers leave the proof mass free in one direction. In the other two directions the motion is completely restricted. The main architecture of this accelerometer type can be seen in Figure 19.

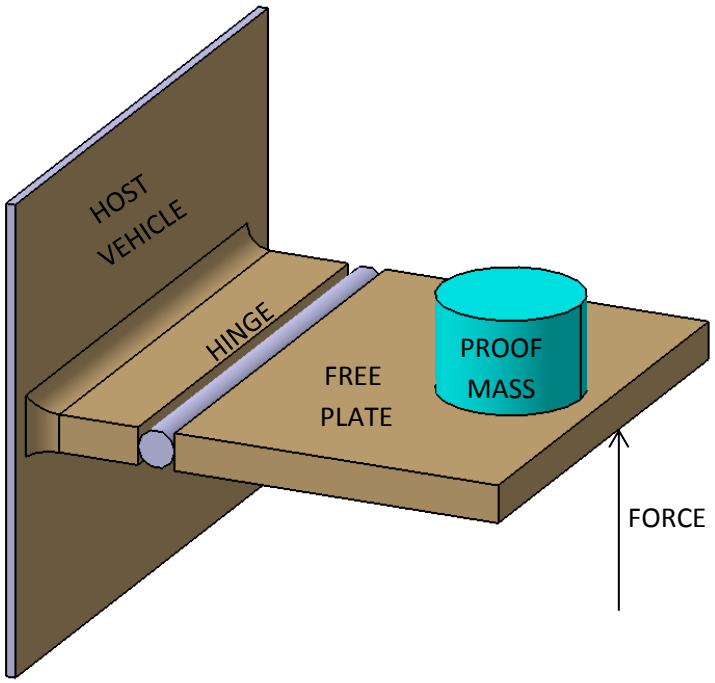

Figure 19: Representation of a pendulous accelerometer.

Pendulous accelerometers measure the force needed to maintain the hinge at 0 degrees. This force is proportional to the acceleration to which the mass is subjected. The hinge is a very important part of the accelerometer. Two types of hinges exist, the flexure and the jewelled pivot hinges. Flexure hinges need very stable materials and it must be verified that the material does not exceed the yield stress during its operation. Furthermore, they have a temperature dependent performance that imposes the need of calibration and temperature data compensation. In contrast, jewelled pivot hinges use two spring-loaded assemblies that do not have temperature dependent performance. Furthermore, they protect the proof mass from shocks. This also implies performance degradation as the input increases. As a result, flexure hinges are used in applications where inputs can be greater than 20 g and jewelled pivot hinges for applications when the input is not expected to reach 20 g.

Electromagnetic accelerometers are a type of pendulous accelerometers. They are characterized by generating the feedback force with a voice coil attached to the free plate. This system, shown in Figure 20, is susceptible to be transformed in a pulse-integrating accelerometer. An electromagnetic accelerometer uses continuous current regulated by a displacement sensor. The displacement sensor usually is a capacitance. The pulse-integrating accelerometer uses very repetitive pulses to maintain the hinge at 0 degrees. Each pulse is generated by a velocity

increment. As in torque feedback gyroscopic accelerometers, the number of pulses is controlled in order to determine the host vehicle velocity.

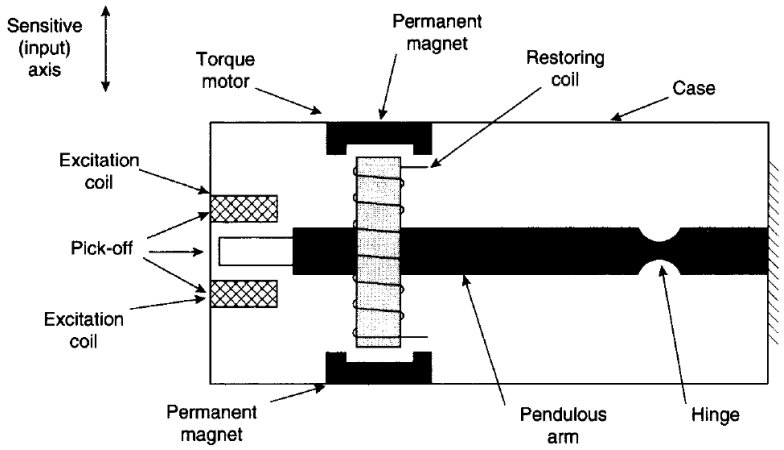

Figure 20: Electromagnetic accelerometer [A-1].

The electromagnetic accelerometer can be modified in order to measure the acceleration in two axes. The proof mass is placed in a plate attached to another plate with a pair of spring hinges. This second plate is attached to the sensor base with a pair of spring hinges perpendicular to the first pair of spring hinges.

The first approximation to open-Loop MEMS accelerometers did not use any hinge. The force that moved the proof mass was applied by the free plate, which in this case was clamped into the MEMS base. In these accelerometers the surface strain was measured with a piezoelectric capacitor or an ion implemented piezo-resistor.

Inside the category of force feedback accelerometers, there is the subcategory silicon accelerometer. They can be MEMS or not. When they are MEMS they have less precision, but they are smaller and lighter.

A.3.4.1 Silicon cantilever accelerometer

This accelerometer consists in a cantilever silicon beam with area reduction near ~~to~~ the fixed part acting as a hinge. The end of the cantilever is gold plated in order to improve the sensor sensitivity and also acts as a proof mass. One cantilever side is metal plated and acts as a capacitor. The other capacitor plate is the silicon substrate. The configuration in closed loop is shown in Figure 21.

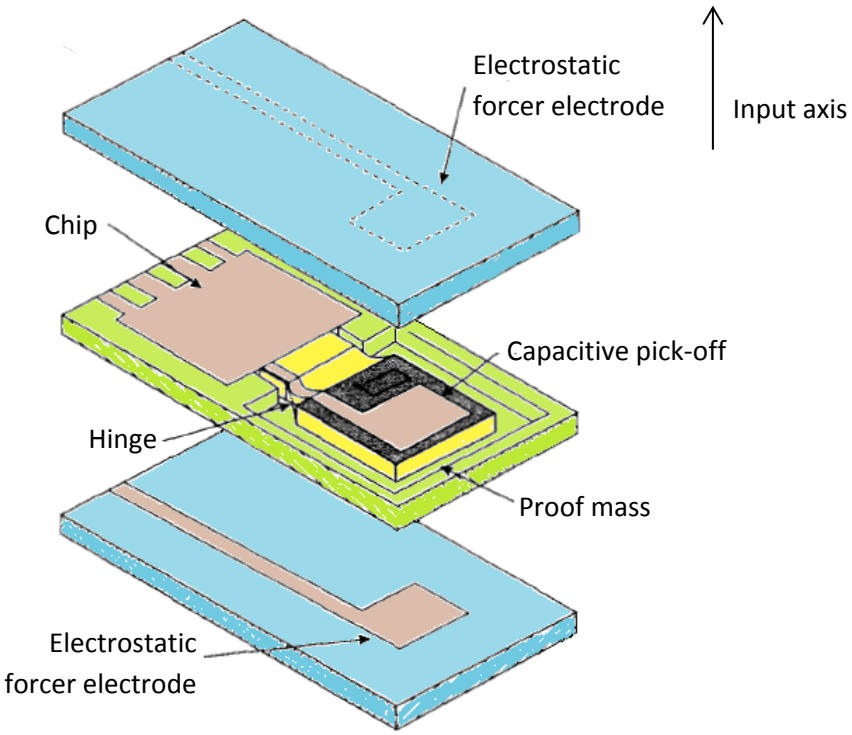

Figure 21 Silicon cantilever accelerometer [A-2].

This configuration can be simplified by using the open loop configuration. In this case, the sensitivity would decrease. By definition, in open loop configuration the capacitance is measured to determine the acceleration but no additional action is done.

Tunnelling MEMS accelerometers have a very similar functioning. The advantage of this MEMS with respect to the previous one is the simplicity of the manufacturing. Therefore, it is cheaper. This accelerometer is a closed-loop sensor. The way this accelerometer works can be seen in Figure 22.

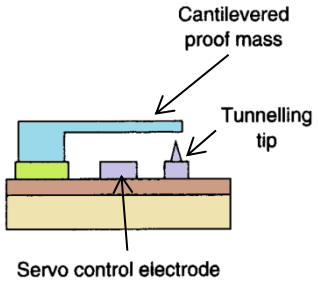

Figure 22: Tunnelling MEMS accelerometer [A-1].

A.3.4.2 Monolithic accelerometer

The monolithic accelerometer is an open-loop accelerometer. A cylindrical monolithic proof mass is placed between two silicon diaphragms with differential capacitive pick-off on each edge.

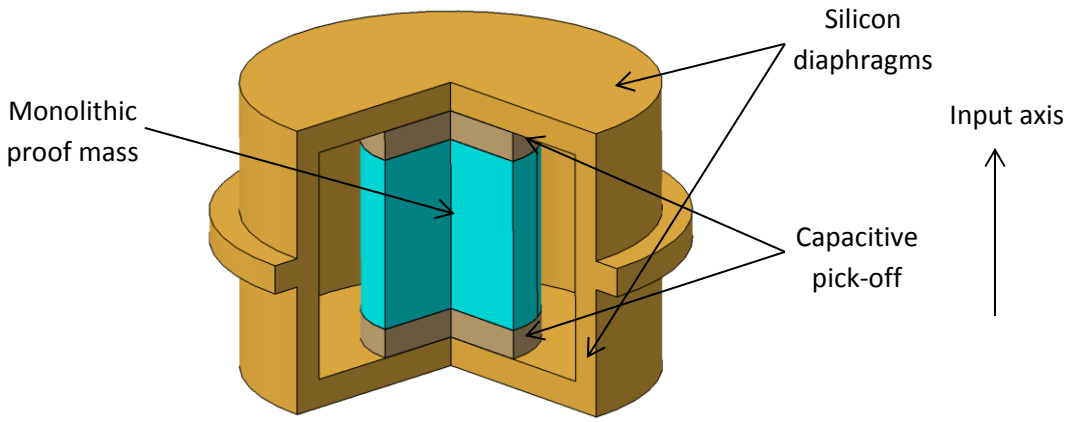

Figure 23: Monolithic accelerometer

This sensor has not been proved in an INS due to the manufacturing difficulties.

A.3.4.3 Resonant silicon accelerometer

This technique uses two bars to suspend a silicon proof mass. These bars are maintained at mechanical resonance with quartz resonators. When the sensor is undergoing acceleration, the proof mass tenses the bars and the vibrating frequency changes. This frequency change is measured and it is proportional to the acceleration.

A.3.5 Surface acoustic wave resonator

The surface acoustic wave resonator uses a pendulum configuration that measures the frequency change in the plate due to accelerations orthogonal to the plane. This configuration is similar to that shown in Figure 19, but without the feedback force and the hinge. Instead of these, it has a pair of electrodes placed at different distances from the edge. The electrodes are used to force a vibration in the plate. When the sensor is accelerated, the plate vibration frequency changes. Then, this frequency is measured in the electrodes.

A.3.6 Optical fibre accelerometers

A.3.6.1 Suspended optical fibre accelerometer

By definition, this sensor is a two axes accelerometer. In this accelerometer an optical fibre is suspended from a solid state laser with a micro-lens and a proof

mass at the other edge. Perpendicular to the array a two-dimensional photo-sensitive array is placed. When an acceleration perpendicular to the optical fibre applies, the optical fibre is deflected. Then, the laser light focusing point is displaced by a distance proportional to the acceleration sensed.

A.3.6.2 Mach-Zehnder interferometric accelerometer

This accelerometer has a proof mass at the end of the optical fibre. When acceleration in the optical fibre occurs, the proof mass tenses or compresses the optical fibre, thus modifying its length. The sensor sensitivity can be increased by placing another fibre at the opposite side of the proof mass. Then, the change in the length of the second optical fibre is equal and opposite to the first fibre length change. The optical fibre length is measured by phase change.

If the performance needs to be improved, the sensor can be implemented in a closed-loop system. The phase change acts upon a piezoelectric cylinder that reduces or increases the length of the optical fibre.

A.3.6.3 Vibrating fibre optic accelerometers

This sensor uses optical fibre tensioned between two rigid supports and vibrating at its natural frequency (*f*). When the signal passes through the vibrating optical fibre, it is phase modulated at frequency *2f* and higher-order even harmonics of *f*. But when the accelerometer is submitted to acceleration, the displacement becomes asymmetric and the signal is also phase modulated at frequency *f* and higher-order odd harmonics of *f*. The odd harmonic phase modulation amplitude is proportional to the sensed acceleration.

A.3.6.4 Photo-elastic fibre optic accelerometers

This accelerometer has a very low Technology Readiness Level (TRL). The photo-elastic material has a proof mass situated in the measurement direction. When the photo-elastic material is compressed due to acceleration, the transitivity changes. This effect is used to measure the acceleration. Commercial use of this sensor is not expected in near future. Therefore, it is not going to be further detailed in this project.

A.3.6.5 Bragg grating fibre accelerometer

Bragg grating avoids the transmission through an optical fibre of a determined wavelength. This wavelength is determined by the Bragg grating design, temperature, strain and pressure. Then, the acceleration can be determined by measuring the signal that has passed through the Bragg grating and by controlling the temperature and pressure.

A.3.7 Vibratory accelerometers

Vibratory accelerometers use the frequency change in a vibration due to acceleration to measure it. This configuration is shown in Figure 24. When one beam is in compression and this frequency is reduced, the other beam is in tension and increases its frequency. This configuration cancels or minimizes the errors originating from temperature changes, ageing of the sensor, factor asymmetry aniso-inertia and other effects.

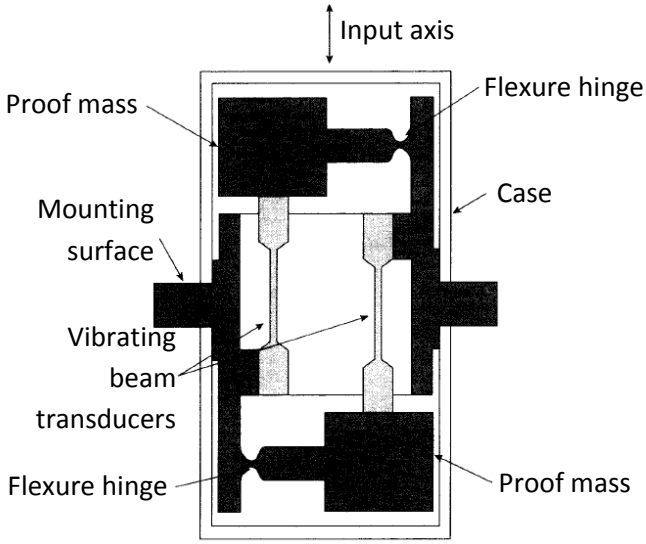

Figure 24: Vibrating accelerometer [A-1].

A.3.8 Angular Accelerometers

In general, accelerometers are less problematic than gyroscopes. As a consequence, the question arises: why do not use accelerometers located away from the ISA to detect rotations around the ISA axes? The threshold of accelerometers and the error time dependency make this design useless for navigation. The accelerometer threshold would permit the launcher to roll at high rates without being detected. Furthermore the error would increase with t^3.

Such systems have been implemented in camera and gun high frequency stabilization systems, where the system drawbacks do not penalize the system performance.

A.4 Specifications overview

Table 1 and Table 2 contain indicative values of some accelerometer and gyroscope specifications. The values have been extracted from reference A-1, A-2 and A-3.

ACCELEROMETER TYPE	Range [g]	Scale-factor stability [%]	Scale-factor non-linearity [%]	Bias [g]	Bias repeatability [g]	Temperature bias [g/^{0}C]	Hysteresis [g]	Threshold [g]	Bandwidth [HZ]
Electromagnetic force feedback accelerometer	100	0.1	0.05	10^{-4}	0.001	0.001	0.002	10^{-5}	400
Vibratory accelerometers	200	0.01	0.05	0.1				10^{-5}	100
Optical fibre accelerometers	20	0.001	0.05	10^{-3}				10^{-6}	100
Surface acoustic wave resonator	100	0.1	0.1	$5\cdot10^{-4}$				10^{-6}	400
Resonant silicon accelerometer	100	0.5	0.1	$2.5\cdot10^{-2}$				10^{-6}	400

Table 1: Specifications overview of some accelerometer types detailed in this annex.

GYROSCOPE TYPE	g-Independent bias [^{0}/h]	g-dependant bias [^{0}/h/g]	Anisoelastic bias [^{0}/h/g^2]	Scale-factor error [ppm/^{0}C]	Scale factor non-linearities [%]	Bandwith [Hz]	Maximum input rate [^{0}/s]	Random walk [^{0}/h$^{0.5}$] / comments
Coriolis gyroscope	0.001						500	
Coriolis torque feedback gyroscope	0.05-10	1-10	1-2	400	0.01-0.1	60	400	
Dynamically tuned gyro	0.05-10	1-10	0.1-0.5	400	0.01-0.1	100	1000	
Flex gyroscope	1-50	1-10	0.05-0.25	400	0.01-0.1	100	500	
DART	0.1-0.4 [^{0}/s]	0.03-0.05 [^{0}/s/g]	0.005 [^{0}/s/g^2]		5	80	800	
Magnetohidrodynamic gyroscope	0.05-0.5 [^{0}/s]	0.05 [^{0}/s/g]	0.001 [^{0}/s/g^2]	4	0.1	100	400	
Hemispherical Resonator gyro	0.01			1 ppm				0.0008
MEMS vibrating disc gyro	0.05 [^{0}/s]			1000 [ppm]	1		1000	0.5 [^{0}/S$^{0.5}$]
Tuning fork gyro	1							
Tuning fork gyro (MEMS)	3-10	10			0.05-0.15		6000	0.01-0.3
Silicon gyro	100							
Vibratory gyroscope	0.1-1 [^{0}/s]			100-500	0.03-0.3	60-500		Shock resistance >25000 g
Electrostatically suspended gyro	0.0001							No shock resistance
Fluxgate magnetometer gyroscope	0.1 ^{0}	0						
ASG	$4\cdot10^{-2}$							$2\cdot10^{-3}$
Ring laser gyroscope	0.001-10	≈0	≈0		0.01	200	1000	0.001
Fiberoptic gyroscope	0.5-50	≈1	≈0.1		0.05-0.5	100	1000	

Table 2: Specifications overview of some gyroscope types detailed in this annex.

A.5 References

A-1 D.H. Titterton, J.L. Weston, *Strapdown Inertial Navigation Technology*, Second Edition 2004

A-2 Anthony Lawrance *Modern Inertial Technology – Navigation, guidance, and control*, Second edition, Springer, 1998

A-3 Mobinder S. Grewal, Lawrance R. Weill, Angus P. Andrews, *Global Positioning Systems, Inertial Navigation, and Integration*, Second Edition, Wiley, 2007

A-4 Nishanthan Rabeendran, *A study of Ring Laser Gyroscopes*, University of Caterbury, 2008

A-5 Advances in Atomic Gyroscopes: A View from Inertial Navigation Applications, JianCheng Fang and Jie Qin (Beihang University)

A-6 Cold Atom Navigation Sensors, Mark Kasevich, Atom Interferometry Group, Stanford Center for Position, Navigation and Time

A-7 Characterization of a cold atom gyroscope, A. Landragin, A. Gauguet ,T. Lévèque, W. Chaibi (Systèmes de Référence Temps-Space – SYRTE).

A-8 Atomic gyroscope: present status and prospective, Arnaud Landragin, Walid Chaibi, Alexandre Gauguet, Thomas Lévêque, Franck Michaud (Systèmes de Référence Temps-Space – SYRTE).